AD-B181 912

CONFIDENTIAL
CONFIDENTIAL

UNCLASSIFIED

0

TM No.
TA11-C22-74

NAVAL UNDERWATER SYSTEMS CENTER
NEW LONDON LABORATORY
NEW LONDON, CONNECTICUT 06320

COHERENCE OF HARMONICALLY RELATED CW SIGNALS (U)

Date: 22 July 1974

Prepared by: G.E. DeVilbiss
G. DEVILBISS
Bermuda Research
Detachment

R. L. Martin
R. L. MARTIN
Ocean Sciences and
Technology Department

N. Yen
N. YEN
Ocean Sciences and
Technology Department

National Security Information
Unauthorized Disclosure Subject to Criminal Sanctions

94-06216

Classified by: Code 102-OSC (ONR)
Subject to GDS of EO 11652
Declassified on 31 Dec 1981.

CONFIDENTIAL
(This page is UNCLASSIFIED).

CONFIDENTIAL

94 2 24 179

UNCLASSIFIED

442 - 0771 - EXT.
AUTOVON 636 + EXT. 2832

IN REPLY REFER TO:
TA11:RLM:bac
3900
Ser TA11-C52

CERTIFIED MAIL
CONFIDENTIAL - UNCLASSIFIED UPON REMOVAL OF ENCLOSURE (1)

31 JUL 1975

From: Commanding Officer
To: Chief, Office of Naval Research (102-OSC), Arlington, VA 22217

Subj: Technical Memorandum; forwarding of (U)

Encl: (1) (C) Tech Memo No. TA11-C22-74 of 22 July 1974

1. (U) Enclosure (1) is forwarded for your information and retention.

2. (U) Enclosure (1) is forwarded to contractors for the duration of their respective contracts. Upon completion of these contracts, the document must be returned to NUSC.

3. (U) Enclosure (1) shows that signals which are coherently related at the source have a slowly varying phase relationship at a receiver and can be coherently summed to provide additional processing gain. Changes in the phase relationship are apparently due to modifications of the multipath structure, but no definitive explanation of this effect was possible with this set of experimental data.

R. W. HASSE
By direction

08832
3 cys w/3 cys Encl (1)
1 cy w/1 cy Encl (1) sent
06 H1-4 (a)
(b)

CONFIDENTIAL

CONFIDENTIAL

TM No.
TA11-C22-74

ABSTRACT

(C) Measurement data from NORLANT '72 exercise for two harmonically related CW signals, 128 Hz and 85 Hz, have been processed to obtain the phase angle relationship between them as a function of time. The results show that the relative phase angle stayed unchanged or varied slowly with time in most cases but fluctuated greatly in the fading zone. The influence on the coherence of these signals due to hydrophone array configurations, noise, and multipath interference is discussed with some theoretical analysis. The technique for measuring the phase angle for the study of coherence relations presents some useful applications.

ADMINISTRATIVE INFORMATION

(U) This memorandum was prepared under Project No. A-650-15, Sub-project No. R2408, (U) "Long Range Acoustic Transmission Experiments for Surveillance Systems Development." The sponsoring activity is Office of Naval Research. The principal investigator is R. W. Hasse, Code TA. The program manager is Dr. R. D. Gaul, Code 102-OS.

(U) The authors of this memorandum are located at the New London Laboratory, Naval Underwater Systems Center, New London, Connecticut 06320.

INTRODUCTION

(C) As part of the NORLANT '72 exercise (reference (1)) the second and third harmonics of a 43 Hz CW signal were simultaneously transmitted from a projector at 91 m depth and, later, from the same projector raised to 18 m at each of three stations in the Labrador Sea located several hundred miles from a receiving array on the Grand Banks. The two signals, propagating over identical paths, were processed at the array output to determine the degree of coherence between them, the change in this coherence with time, and to investigate the effects of source and array parameters and ocean medium on the coherence. The results are analyzed to compare with the theoretical relations. The processing gain, by utilizing the coherence relation for various propagation conditions is computed. The technique for measuring the phase information presents some potential applications.

BACKGROUND

(C) Coherence of acoustic signals under various propagation conditions in the ocean environment has been of great interest in the development of long range underwater detection and communication systems. There are many environmental parameters such as anisotropic properties of the medium and the condition of surface and bottom boundaries which cause fluctuation of acoustic signal along its transmission path. Studies have been conducted in the past for the purpose of relating the space coherence of the received signals at various distances with environmental parameters. For example, Robertson and Wagner (reference (2)) have reported coherence measurements at an array due to signals transmitted by a CW source suspended from a freely drifting ship, and more recently, Beam (reference (3)) reported work on phase fluctuations for a signal transmitted from a CW source towed radially at 10 knots. The results of these studies have been used in the understanding of the maximum achievable array gain under actual ocean environments. On the other hand, little work has been done regarding the environmental influence on the combination of signals transmitted along the same path. A particular example is the harmonically related CW signals which possess certain initial relationships among their phase angles. When a combination of such signals propagates through the ocean medium, the phase angle relationships will be modified due to different responses of the environmental parameters to each harmonic component.

Tucker and Barnickle (reference (4)) have applied the stability of such phase relationships to identify underwater objects by employing harmonically related CW signals. If the phase relationships of harmonically related signals propagating over long distances are stable in time it is possible to bandshift one signal to the frequency of the other and to coherently sum them to obtain a processing gain between 0 and 3 dB.

(U) For two signals with amplitudes of A and B, and a relative phase angle of ϕ, the coherence gain is defined as:

$$G = 10 \log \left[\frac{(A^2 + B^2 + 2A \cdot B \cos \phi)}{A^2 + B^2} \right],$$

$$= 10 \log \left[1 + \frac{2A \cdot B}{A^2 + B^2} \cos \phi \right], \tag{1}$$

where the second term in the brackets is the cross-correlation of the two signals. When A=B, the maximum coherent gain will be achieved and Equation (1) can be rewritten as

$$G_{max} = 10 \log [1 + \cos \phi]. \tag{2}$$

When ϕ is a time variable, the average gain will be

$$\overline{G_{max}} = 10 \log \left\{ 1 + \text{avg.} [\cos \phi(t)] \right\}. \tag{3}$$

In the general case of more than two signals, Equation (3) has the form

$$\overline{G_{max}} = 10 \log \left[1 + \sum_{ij} \text{avg.} (\overline{\rho_{ij}}) \right], \tag{4}$$

Where ρ_{ij} is the correlation between the ith and jth signals.

CONFIDENTIAL

MEASUREMENTS

(C) The NORLANT '72 exercise was conducted in the Labrador Basin during July and August 1972. The exercise was intended to provide an assessment of the surveillance potential in the Labrador Basin and to serve as the basis for more extensive operation at a later date. A preliminary report of the exercise has been published by Martin and Adams (reference (5)).

(C) Measurement of coherence of harmonically related CW signals was performed during the period 20 July to 24 July 1972. A CW projector was deployed by USNS SANDS first to a depth of 18 m for several hours and then to 91 m for approximately the same length of time at sites shown in Figure 1. During deployment periods, SANDS was allowed to drift. The signals were received several hundred miles away at a hydrophone array on the Grand Banks.

(C) The signal source was operated simultaneously with harmonically generated CW signals with intensity of 189 dB//μPa at frequencies of 85.47 and 128.205 Hz which correspond to second and third harmonics of 42.735 Hz respectively. These exact values of the frequencies resulted from electronically dividing down from a stable oscillator (1 part in 10^8/day) at 120 kHz. The second and third harmonics were chosen so that the two frequencies would be near the maximum mechanical response of the HX 231 sound source used; this resonance frequency was 104 Hz. The HX 231 bender bar projector was lowered to 91 m and operated in a continuous mode the last 55 minutes of each hour for several hours at each of three sites. After each 91 m operation, the source was raised to 18 m and the process repeated. Station positions and operating times at each depth are given in Table 1. The data were collected on magnetic tape at single hydrophones and beam outputs of the array. The received level was not adequate for processing using single hydrophone recordings but the narrowband signal-to-noise ratio at the beam output was sufficient.

DATA PROCESSING

(C) Figure 2 is a block diagram of the system used to process the data recorded on the magnetic tape. The signals were processed through two separate channels; one channel contained a digital filter (reference (6)) of 128 Hz center frequency and 0.24 Hz bandwidth followed by **a bandpass active filter to reduce** the aliasing frequency components and the other contained a digital filter with center frequency of 85 Hz and bandwidth of 0.24 Hz. The center frequencies of the digital filters were set by a frequency synthesizer and the drift of the center frequency relative to the third harmonic signal was continuously monitored using a phase meter and strip chart recording to ensure the proper setting of the synthesizer. The 85 Hz second harmonic signal was bandshifted to the third harmonic frequency near 128 Hz by going through a squarer clipper, frequency divider (x 1/2), and a band pass active filter to isolate the third harmonics. The outputs of these two channels fed a phase meter for comparing their phase. The time series of the resulting relative phase was plotted continuously on a strip chart.

(U) A phase reversal switch was provided at the input of the phase meter so when the phase angle difference approached 360 degrees, a known 180 degree shift could be induced by simply reversing the polarity of one of the signals thereby keeping the plotted result near the center of the chart; a note is made on the strip chart whenever such a change is made.

(C) The amplitudes vs. time of the 128 and 85 Hz signal components at the output of the active filters were recorded on two channels of a separate Sanborn recorder.

(C) The noise levels at both signal channels were obtained when the signal was off. The signal-to-noise ratio thereafter was established by monitoring the output level of the two signals.

(U) Doppler shift due to the drift of the source ship was deduced from the phase angle relatinn between the 128 Hz recorded signal and the 128 Hz reference. It was observed that the shift in phase between these two signals was almost constant during the measurement period. The drift velocity of the source (normal component) can be estimated by the relation

$$V_S = \left(\frac{\frac{2\pi}{T}}{128} \right) \cdot c \, ,$$

where T is the period in seconds for a total 360 degrees of phase shift and c is the average speed of sound in the medium.

UNCLASSIFIED

CALIBRATION

(U) Signals from two frequency synthesizers, differing by a few tenths of a Hertz from each other were used to calibrate the phase response of the system. The constant change in relative phase of these two signals result in a ramp voltage corresponding to a range of 0 to 360 degrees in phase. Full scale on the chart corresponds to a total of 360 degrees and the slope of the line indicates the linearity of phase response. A 6 volts peak to peak signal amplitude at the input to the digital filters was found to be the upper voltage limit for obtaining a linear phase response of the system.

(U) The response of the system has also been checked with noise added to the signal. The distribution of phase angle was recorded at various signal-to-noise ratios. The result was used to compute the coherence gain using Equation (3). The data are plotted in Figure 4 for comparison with the expected performance of the system.

THEORETICAL ANALYSIS

(U) RELATIVE PHASE ANGLE BETWEEN TWO HARMONICALLY RELATED SIGNALS:

a propagating CW signal can be represented by:

$$S_o = A_o \sin\left[\omega_c(1+\delta_o)t - k_o x + \phi_o\right], \qquad (5)$$

where
A_o = Amplitude
ω_o = Angular Frequency
k_o = Wave Number $\left(\frac{2\pi}{\lambda_o}\right)$
ϕ_o = Phase Angle
x = Range

UNCLASSIFIED

UNCLASSIFIED

$$\delta_0 = \frac{C + V_m - V_r}{C + V_m - V_s} \text{ (Doppler Shift)}$$

C, V_m, V_r, and V_s are velocity of sound in the medium, velocity of medium, velocity of receiver, and velocity of the source respectively. For two harmonically related signals, one with angular frequency of $\omega_m = m\omega_0$ and the other with frequency $\omega_n = n\omega_0$,

$$S_m = A_m \sin\left[\omega_m(1+\delta_m)t - k_m x + \phi_m\right],$$

$$\text{and} \quad S_n = A_n \sin\left[\omega_n(1+\delta_n)t - k_n x + \phi_n\right]. \tag{6}$$

If S_n is shifted to the same frequency band as S_m, the difference in phase angle between these two signals will have the form:

$$\Delta\phi = \Big[\omega_m(1+\delta_m)t - \frac{m}{n}\omega_n(1+\delta_n)t - k_m x + \frac{m}{n}k_n x + \phi_m - \frac{m}{n}\phi_n\Big]. \tag{7}$$

Because both signals are transmitted and received by the same projector and hydrophone respectively, and if the medium is non-dispersive for the frequency range of the two signals, then Equation (7) can be simplified to:

$$\Delta\phi = \left(\phi_m - \frac{m}{n}\phi_n\right), \tag{8}$$

where the ϕ's are frequency independent phase changes along the transmission path. The surface reflection which causes 180° phase shift for all signal components is one of the examples of frequency independent phase change. Equation (8) indicates that, if the frequency independent phase change is not a function of distance, the phase difference between two harmonically related signals will not be a function of distance either.

UNCLASSIFIED

TM No.
TA11-C22-74

(U) When the received signal is obtained at the output sum of the hydrophone array, the additional phase difference to be considered is given as:

$$\Delta\phi_H = \tan^{-1}\left\{\frac{\sum_{i=1}^{N-1} W_i \sin[k_m d_i \cos\theta]}{\sum_{i=1}^{N-1} W_i \cos[k_m d_i \cos\theta]}\right\} - \frac{m}{n}\tan^{-1}\left\{\frac{\sum_{i=1}^{N-1} W_i \sin[k_n d_i \cos\theta]}{\sum_{i=1}^{N-1} W_i \cos[k_n d_i \cos\theta]}\right\}, \qquad (9)$$

where

W_i = Shading Factors

d_i = Hydrophone Spacings (distance to the reference hydrophone)

θ = Signal Arrival Angle at Array

For equally spaced array with no shading factor, Equation (9) can be reduced to:

$$\Delta\phi_H = \frac{(N-1)}{2}(k_m d \cos\theta) - \frac{m}{n}\frac{(N-1)}{2}(k_n d \cos\theta), \qquad (10)$$

and the additional phase difference will be cancelled out for the non-dispersive medium due to the fact $k = \omega/c$. Hence the relation concluded from Equation (8) will still be true. However, for the shaded array or an unequally spaced array, the relative phase will be changed due to the different arriving angle of the received signals. The deviation of the resultant phase angle difference can be computed according to the relation expressed by Equation (9). For an array which has a symmetrical configuration, if no shading factor is applied to its hydrophone elements, the phase angle difference caused by different signal angles is zero according to Equation (9).

(U) NOISE INTERFERENCE

(U) Fluctuation of phase angle for a received acoustical signal is generally observed due to noise interference. To analyze the resultant effect on the relative phase of the harmonically related signals plus independent noise, the probability density function of phase angle distribution can be derived.

(U) For simplifying the mathematical operation, we let the reference phase of the signal be zero initially and express the signal with added noise as:

$$
\begin{aligned}
S &= A_o \cos \omega_o t + \sum_n C_n \cos(\omega_n t + \phi_n) , \\
&= \left\{ A_o + \sum_n C_n \cos\left[(\omega_n - \omega_o)t + \phi_n\right] \right\} \cos \omega_o t \qquad (11) \\
&\quad + \left\{ \sum_n C_n \sin\left[(\omega_n - \omega_o)t + \phi_n\right] \right\} \sin \omega_o t ,
\end{aligned}
$$

where

A_o = Amplitude of the Signal

ω_o = Signal Angular Frequency

C_n = Noise Amplitude of Frequency Component at ω_n

ϕ_n = Phase Angle at Noise Frequency Component at ω_n

By assuming the noise to be a Gaussian random process, the probability distribution of the amplitude of the real and quadrature components for the signal plus noise (reference (7)) is:

$$p(x) = (2\pi N)^{-\frac{1}{2}} \exp\left[-\frac{(x-A_0)^2}{2N}\right],$$

$$p(y) = (2\pi N)^{-\frac{1}{2}} \exp\left[-\frac{y^2}{2N}\right], \tag{12}$$

where N = noise power in the passband.

By changing the variables:

$$\begin{aligned} x &= R\cos\phi, \\ y &= R\sin\phi, \\ \phi &= \tan^{-1}\left(\frac{y}{x}\right), \end{aligned} \tag{13}$$

the probability density of the resulting phase angle will be:

$$\begin{aligned} p(\phi) &= \int_0^\infty p(R\cos\phi)\cdot p(R\sin\phi)\,R\,dR, \\ &= \frac{1}{2\pi N}\int_0^\infty \exp\left[-\frac{1}{2N}(R^2+A_0^2-2RA_0\cos\phi)\right] R\,dR, \\ &= \frac{1}{2\pi}\left\{ e^{-(SNR)} + \sqrt{\pi(SNR)}\cos\phi \right. \\ &\qquad \left. \times\left[1+\operatorname{erf}(\sqrt{(SNR)}\cos\phi\right] e^{-(SNR)\sin^2\phi} \right\}, \end{aligned} \tag{14}$$

where (SNR) stands for signal to noise ratio. Curves in Figure 3 show the phase angle distribution at various signal to noise ratio. For signals having large SNR, Equation (14) can be approximated as:

$$p(\phi) = \frac{\sqrt{(SNR)}\cos\phi}{\sqrt{2\pi}} \exp\left[-(SNR)\sin^2\phi\right], \tag{15}$$

UNCLASSIFIED

and can be further reduced for a phase angle distribution near the reference value (the mean of the distribution).

$$p(\phi) = \frac{1}{\sqrt{2\pi}\,\sigma} \exp\left[-\frac{\phi^2}{2\sigma^2}\right], \tag{16}$$

where

$$\sigma = \left[\frac{1}{2(SNR)}\right]^{\frac{1}{2}}.$$

Equation (16) is a Gaussian distribution. The probability density function for phase angle difference between two signals is obtained by consideration of Equation (8).

$$p(\Delta\phi) = \frac{1}{\sqrt{2\pi}\,\sigma_d} \exp\left[-\frac{(\Delta\phi - M)^2}{2\sigma_d^2}\right], \tag{17}$$

where

$$\sigma_d^2 = \sigma_m^2 + \sigma_n^2,$$

$$M = \phi_m - \frac{m}{n}\phi_n,$$

if

$$(SNR)_m = (SNR)_n = (SNR),$$

$$\sigma_d^2 = \frac{1}{(SNR)}.$$

The relation in Equation (17) can be utilized to compute the coherent gain derived in Equation (3). For two equal amplitude signals, the coherent gain in dB is given by Equation (3):

$$G = 10 \log\left[1 + \overline{\cos(\Delta\phi)}\right]$$

UNCLASSIFIED

where upper line designates the average value. Since the probability density function of $\Delta\phi$ is given in Equation (17), the average value of cos ($\Delta\phi$) can be derived:

$$\begin{aligned} \text{Avg.}(\cos\Delta\phi) &= \int_{-\pi}^{\pi} \cos\phi \; p(\phi)\, d\phi , \\ &= \frac{2}{\sqrt{2\pi}\,\sigma_d} \int_{0}^{\pi} \cos\phi \; e^{-\frac{(\phi-M)^2}{2\sigma_d^2}} d\phi , \\ &\approx e^{-\frac{\sigma_d^2}{2}} . \end{aligned} \tag{18}$$

Figure 4 shows the coherent gain as a function of signal to noise ratio. Here it has been assumed that the signal to noise ratio for both harmonically related signals are the same. A more general result could be derived directly from Equation (14); however, a simple closed form just to illustrate the relationship is not easy to obtain.

(U) MULTIPATH EFFECT

(U) If the receiving hydrophone is not highly directional, the signals for comparing the phase difference are actually the results of multipath propagation. To illustrate the multipath effect on the coherence of harmonically related signals, the relationship of a signal formed by propagation over two paths are considered:

$$S_{AB} = A\cos(\omega t - kx_A + \alpha) + B\cos(\omega t - kx_B + \beta), \tag{19}$$

where x_A , x_B are travel distances along two different paths and α, β are their corresponding phase change. The resulting signal will have a phase angle expressed by:

$$\phi_{AB} = \tan^{-1} \frac{\sin(kx_A + \alpha) + \gamma \sin(kx_B + \beta)}{\cos(kx_A + \alpha) + \gamma\cos(kx_B + \beta)}, \tag{20}$$

where $\gamma = B/A$. If $A \geq B$, γ will have a value between 0 and 1.

For the case $\gamma = 1$ (A and B are at the same amplitude).

$$\phi_{AB} = \frac{1}{2}\left[k(x_A + x_B) + (\alpha + \beta) \right] . \tag{21}$$

Equation (21) indicates that the phase change due to the two different travel paths will not enter the relative phase difference through Equation (8). For cases of $\gamma \neq 1$, Equation (20) can be rewritten in the form of:

$$\begin{aligned} \phi_{AB} &= (kx_A + \alpha) + \frac{\gamma}{2}(kx_B - kx_A + \beta - \alpha) + \Delta\phi_{AB} , \\ &= k\left[(1 - \frac{\gamma}{2}) x_A + \frac{\gamma}{2} x_B \right] \\ &\quad + \left[\alpha(1 - \frac{\gamma}{2}) + \beta \right] + \Delta\phi_{AB} , \end{aligned} \tag{22}$$

where $\Delta\phi_{AB}$ is the deviation from the linearization and is plotted in Figure 5. Those curves indicate for $[kx_B - kx_A + \beta - \alpha] < 130°$, the angular deviation is small. Consequently, multipath effect will cause little change in phase angle.

(U) Generalization of Equation (20) for more than two paths can be easily extended to:

$$\phi = \tan^{-1} \frac{\sin(kx_0 + \alpha_0) + \sum_{i=1}^{n} \gamma_i \sin(kx_i + \alpha_i)}{\cos(kx_0 + \alpha_0) + \sum_{i=1}^{n} \gamma_i \cos(kx_i + \alpha_i)} . \tag{23}$$

A simple interpretation of Equation (23) is difficult. However, in general, there are only a few dominant modes in the actual ocean environment at a given propagation range (that is $1 > \gamma_1 > \gamma_2 \cdots$); a general tendency of the phase change can be estimated from Figure 5.

UNCLASSIFIED

(U) In the fading zone, two strong signals of equal amplitude with opposite phase will result in cancellation. The final phase angle of the resulting signal will be contributed by the third or higher modes which will present a sudden change in phase angle. However, the signal-to-noise ratio is usually poor in the fading zone and, therefore, the coherence of the harmonically related signals will be severely influenced by noise.

RESULTS AND DISCUSSIONS

(U) Coherence gain as defined in Equation (3) is computed from the measurement data. The results for various conditions of signal-to-noise ratio is plotted in Figure 4 for comparison with theoretical values. The difference between two sets of curves may be attributed to the approximation of Equation (14) by Equation (16).

(U) Typical time series of the relative phase from the reduced data are shown in Figure 6. (A) is the case when the phase stays almost constant in that particular time interval and S/N is high. (B) shows a slow monotonic phase change with time while in (C) there are large phase angle fluctuations and a shift in the time interval. Case (A) corresponds to the ideal condition discussed in the analysis; high signal to noise ratio and no multipath interference so a constant phase results. Case (C) occurred typically at fading zones when the signal to noise ratio became low. At that particular range, noise caused large fluctuations in phase angle and a change in the dominate multipath modes caused a sudden phase angle shift. There is no simple explanation for the slow drift phenomenon indicated in Case (B). It may be due to slowly changing multipath interference during that time period but there are no data to verify this.

UNCLASSIFIED

(C) Long term phase angle variation during the entire measurement period at the three measurement sites for 91 m and 18 m source depths are shown in Figures 7, 8, and 9. The corresponding signal level of 128 Hz and 85 Hz as well as the rate of phase angle change are also plotted in the diagram with the same time axis. The total range of phase change exceeds 360 degrees in some cases which is more or less dependent on how the ship drifts and the propagation condition. There is some indication that the rate of phase change is closely related to the signal level.

(C) The normal component of ship drift speed can be estimated from the periodic phase change resulting from the comparison of the 128 Hz signal and 128 Hz reference signal. From the reduced data, the calculated value has a range of 1 to 3 knots. The average ship drift speed can also be determined from the starting position and ending position during operation by means of satellite navigation. Those values seem to have a reasonable agreement.

SUMMARY

(U) Studies of the theoretical relations of harmonically related CW signals reveal that the fluctuation in their relative phase angle caused by linear frequency dependent parameters can be eliminated. In an ideal simple propagation condition with only one dominant path mode and on omnidirectional hydrophones, the resulting relative phase angle between two signals will stay constant regardless of movement of transmitter or receiver platform and of the distance between them. When multipath signals are presented or shading of an unequally spaced hydrophone array is used, the situation concerning the relative phase becomes complicated. However, it may be possible to trace the basic relation numerically using computer ray trace programs for detailed analysis.

(C) Measurement from NORLANT '72 exercise for two harmonically related CW signals, 128 and 85 Hz, generally confirmed the theoretical relations. The relative phase angle stayed unchanged or varied slowly in most cases but fluctuated greatly in the fading zone due to low signal-to-noise ratio resulting from multipath inteference. No general conclusion is reached concerning the long term slow phase change. Further investigation is desirable to achieve a satisfactory explanation.

(U) The method used to analyze the phase angle relation from the measurement data provides a new technique to recover the phase information of a signal propagating through the medium. Potential applications of such techniques in target identification and determination of the characteristic of the medium can be easily extended.

REFERENCES (U)

1. NORLANT '72 (C) Phase 1 Operation Plan.

2. G. H. Robertson and R. L. Wagner, " (U) Low-Frequency Coherence Measurements for Long Range Underwater Paths," U. S. Navy Journal of Underwater Acoustics, Vol. 12, No. 2, April 1962, page 427.

3. J. Beam, (C) "Amplitude and Phase Fluctuations for a Signal Transmitted from a Ship-Towed CW Source," NUSC Technical Report 4681, 1974.

4. D. G. Tucker and N. J. Barnickle, (U) "Distinguishing Automatically the Echoes from Acoustically 'Hard' and 'Soft' Objects," J. Sound Vib., 9, 3, page 393-397, 1069.

5. B. B. Adams and R. L. Martin, (C) "NORLANT '72 Preliminary Report," Vol. I and II.

6. L. V. Gibbs, (ZL2AVF) (U) "Digital Filters," QST, April 1971.

7. S. O. Rice, (U) "Mathematical Analysis of Random Noise," BSTJ, 23 and 24.

8. W. B. Davenport and W. L. Root, (U) "Introduction to Random Signal and Noise," New York, McGraw-Hill, 1958.

TM No.
TA11-C22-74

TABLE 1

STATION POSITION

Station	Source Depth	Time *	Position *
1	91 m	201505Z	55°50.0'N, 43°28.1'W
		201755Z	55°48.9'N, 43°26.2'W
	18 m	202005Z	55°48.0'N, 43°24.8'W
		210100Z	55°46.2'N, 43°21.5'W
3	91 m	221305Z	55°38.9'N, [illegible]°[illegible].4'W
		221806Z	58°40.6'N, 38°36.8'W
	18 m	221905Z	58°40.8'N, 38°37.9'W
		230100Z	58°43.3'N, 38°38.6'W
4	91 m	240119Z	55°49.2'N, 33°59.8'W (Est).
		240240Z	55°50.4'N. 34°00.5'W

* The first time and position for each source depth refers to the start of the source operation and the second time to the end of the source operation period.

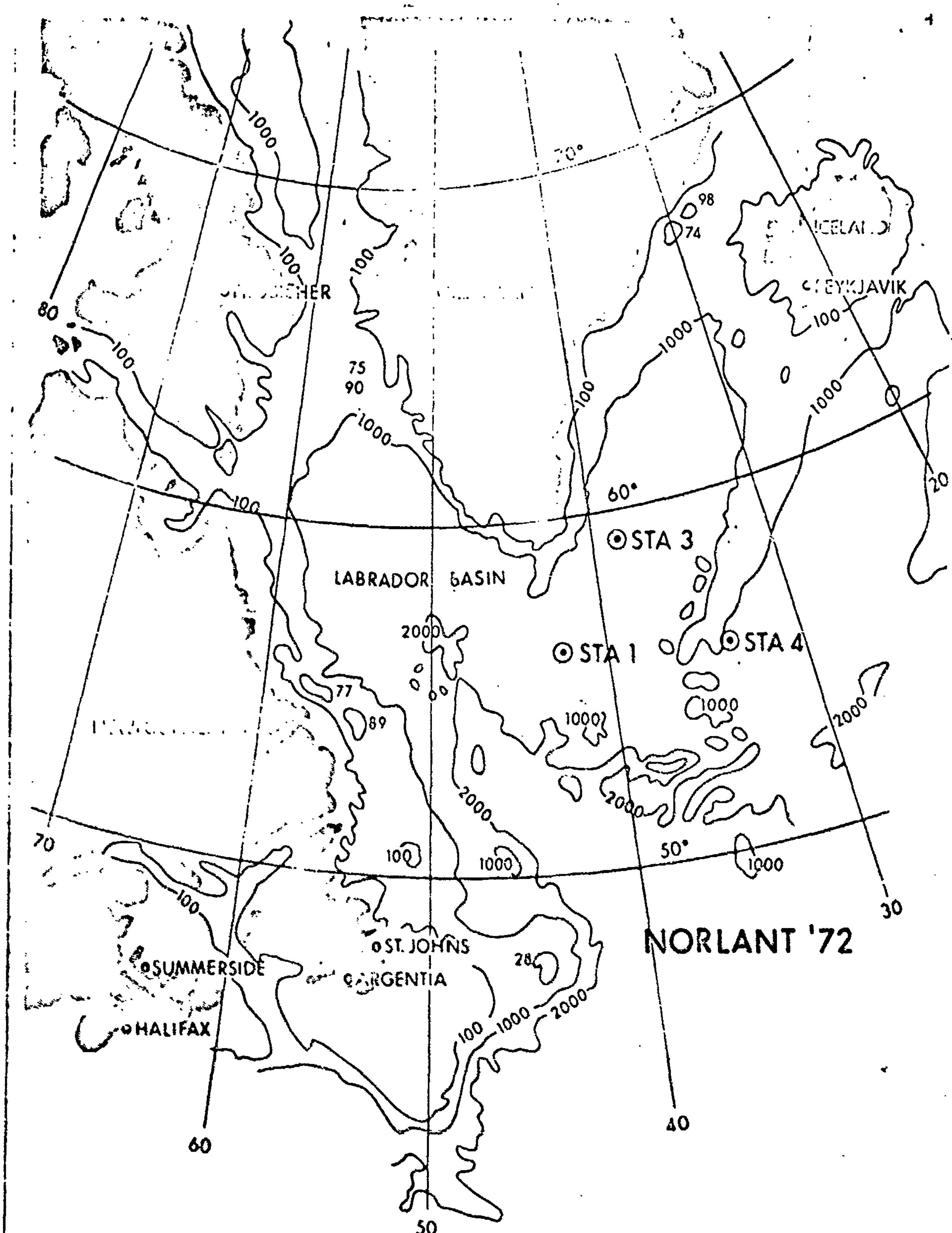

Fig 1. - Measurement Sites

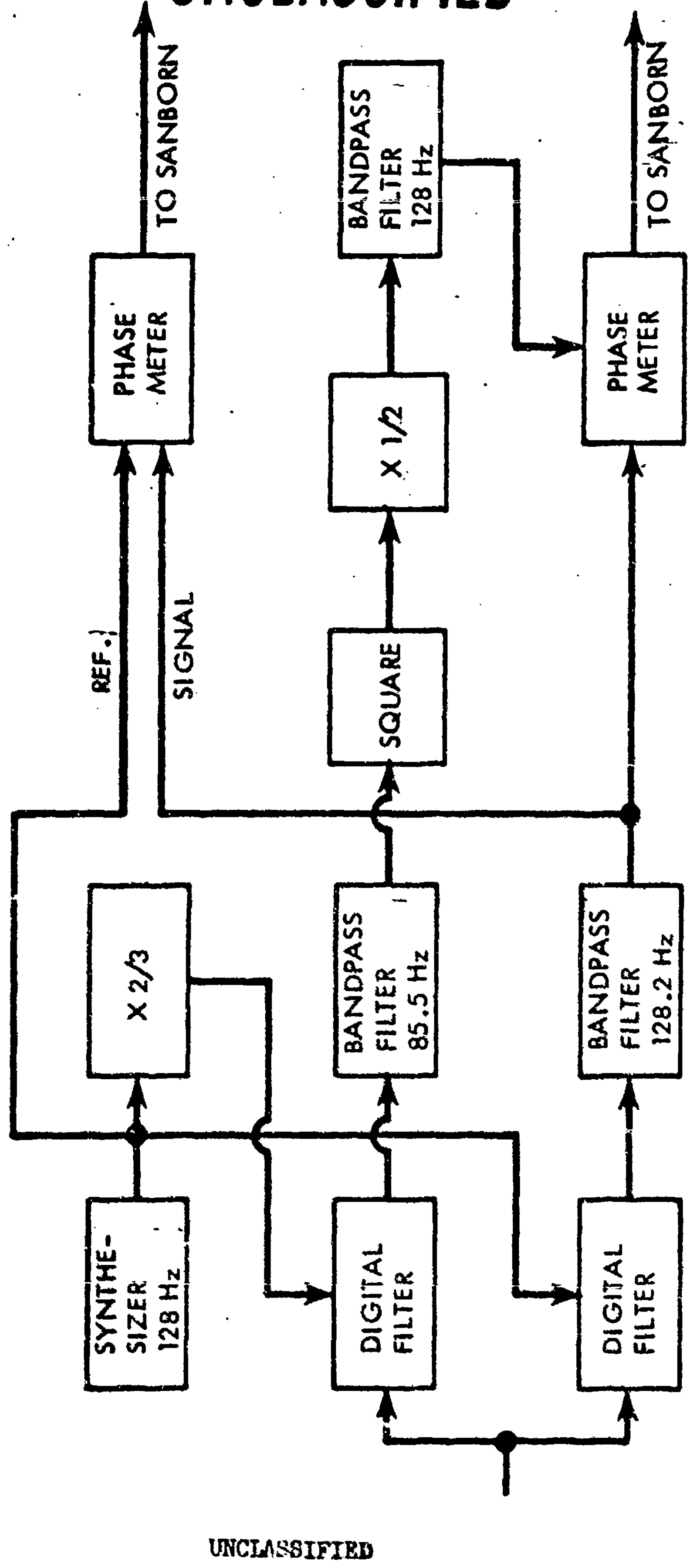

Fig 2. - Block Diagram of Data Reduction System

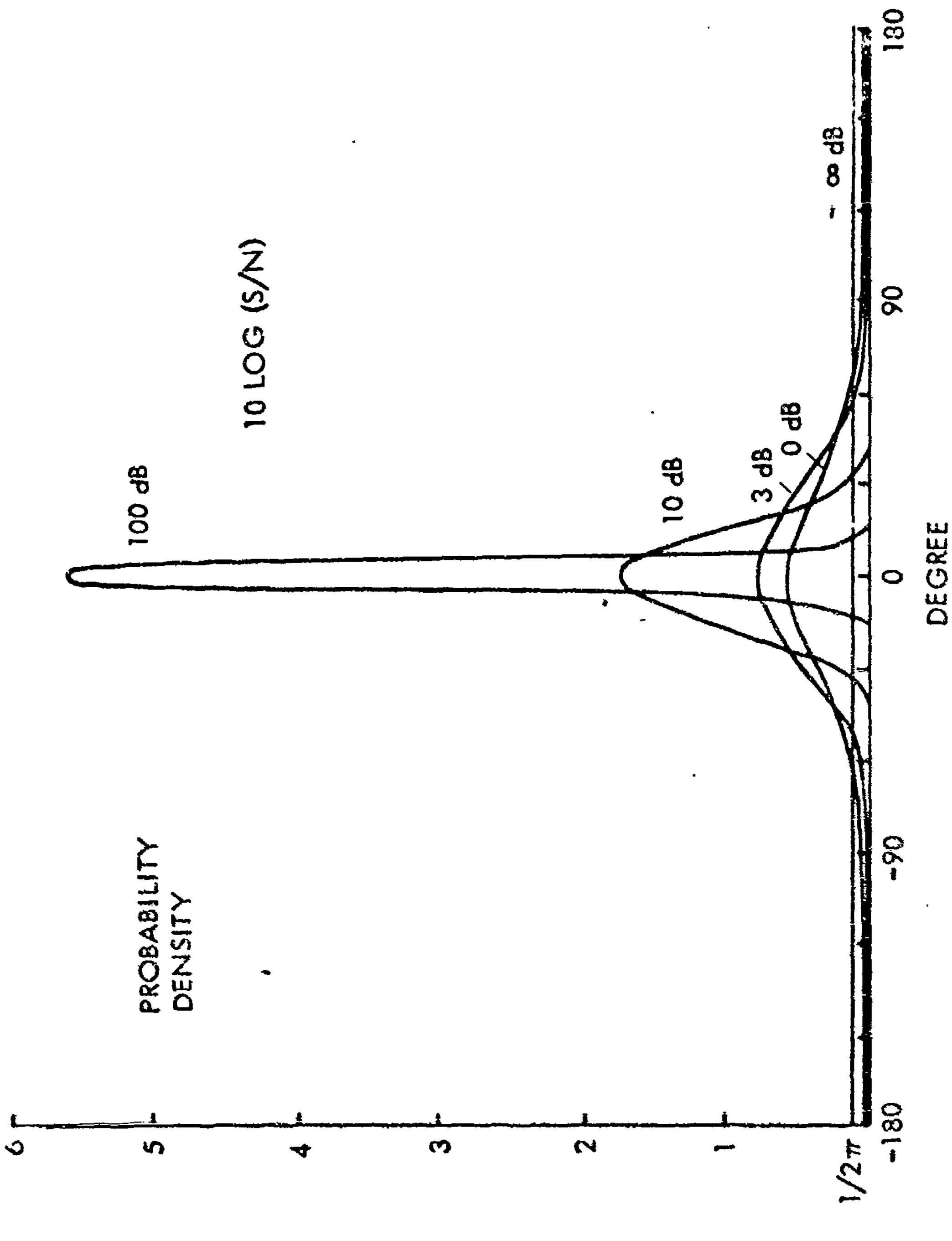

Fig 3. - Phase Angle Distribution at Various Signal to Noise Ratio

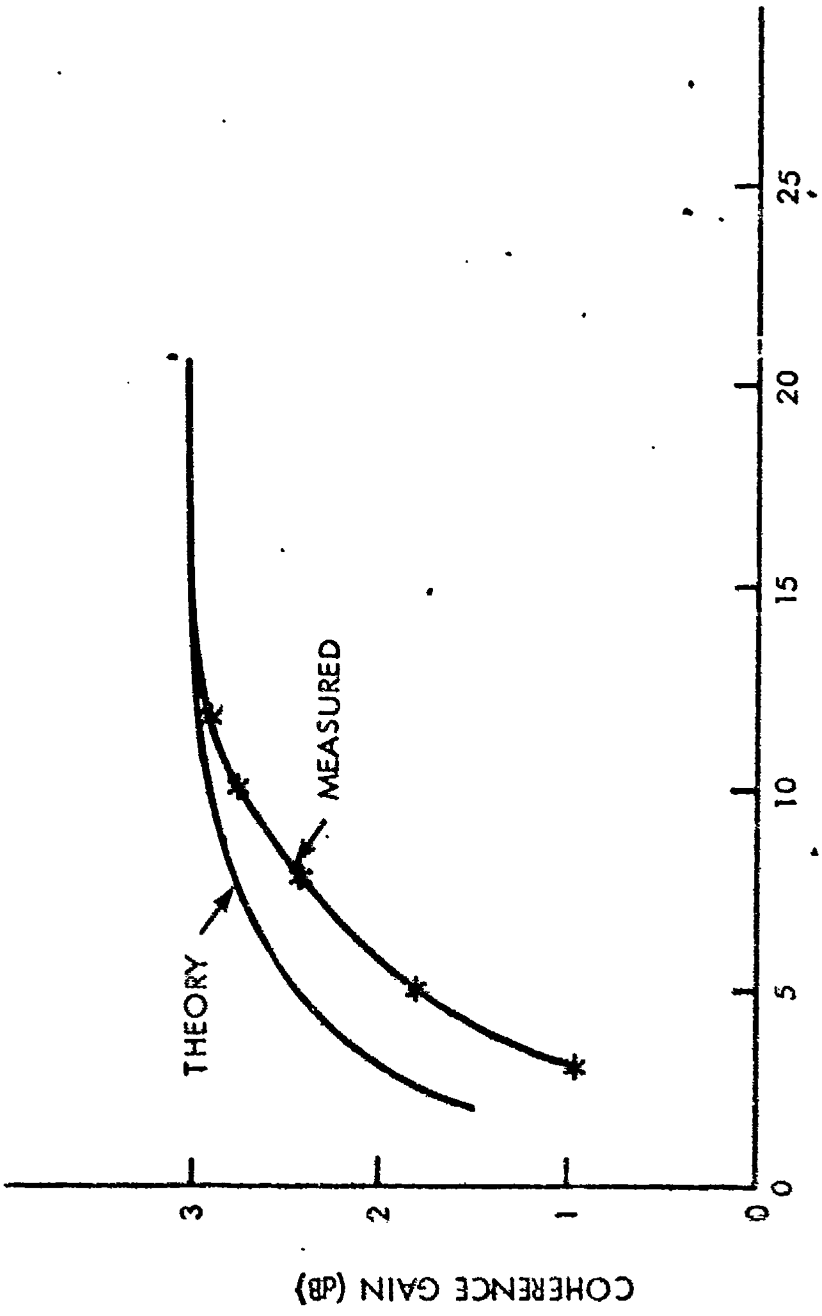

Fig 4. - Coherence Gain as a Function of Signal to Noise Ratio

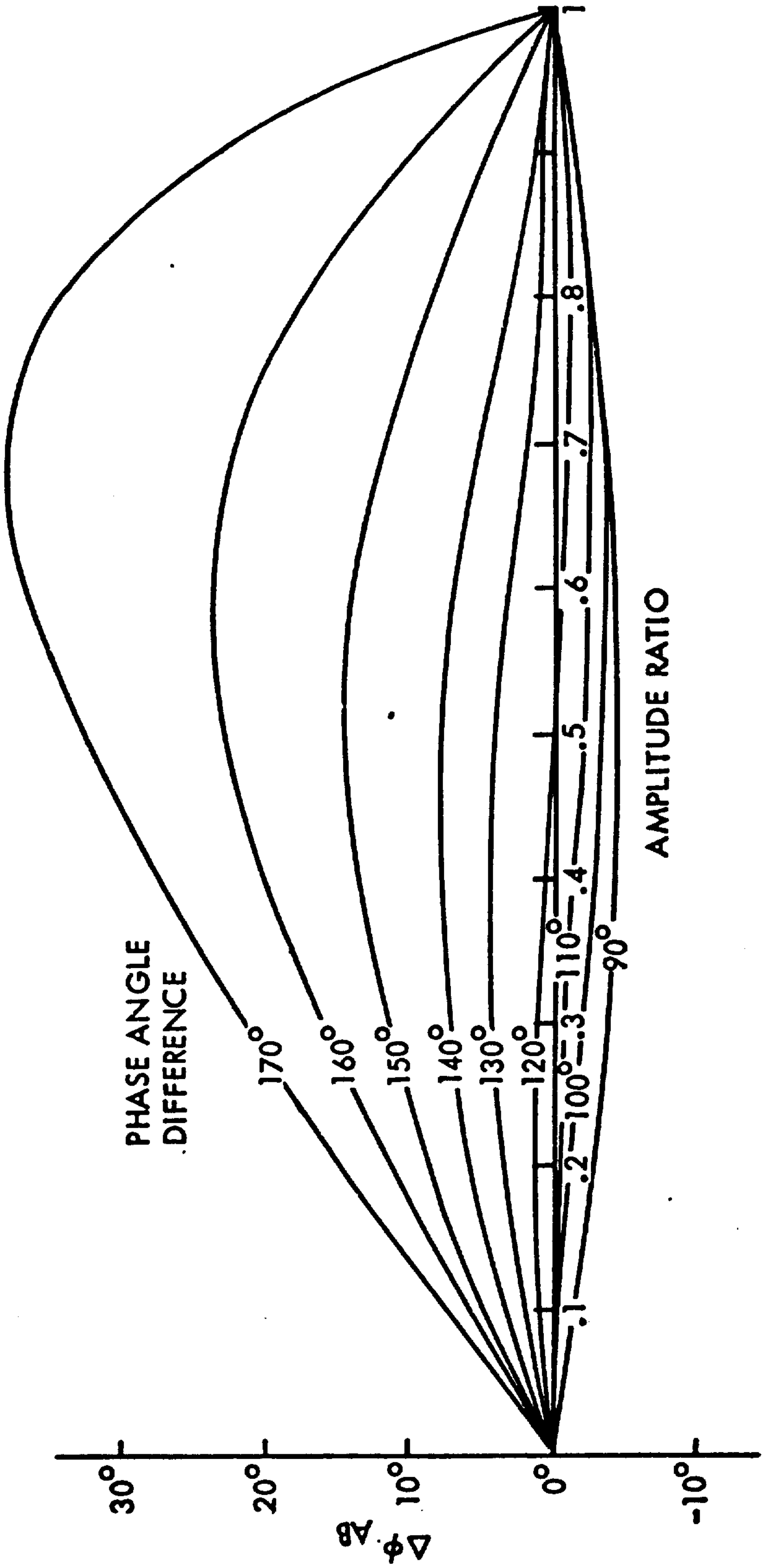

Fig 5. - Phase Angle Deviation from Linearization of Two Coherent Signals

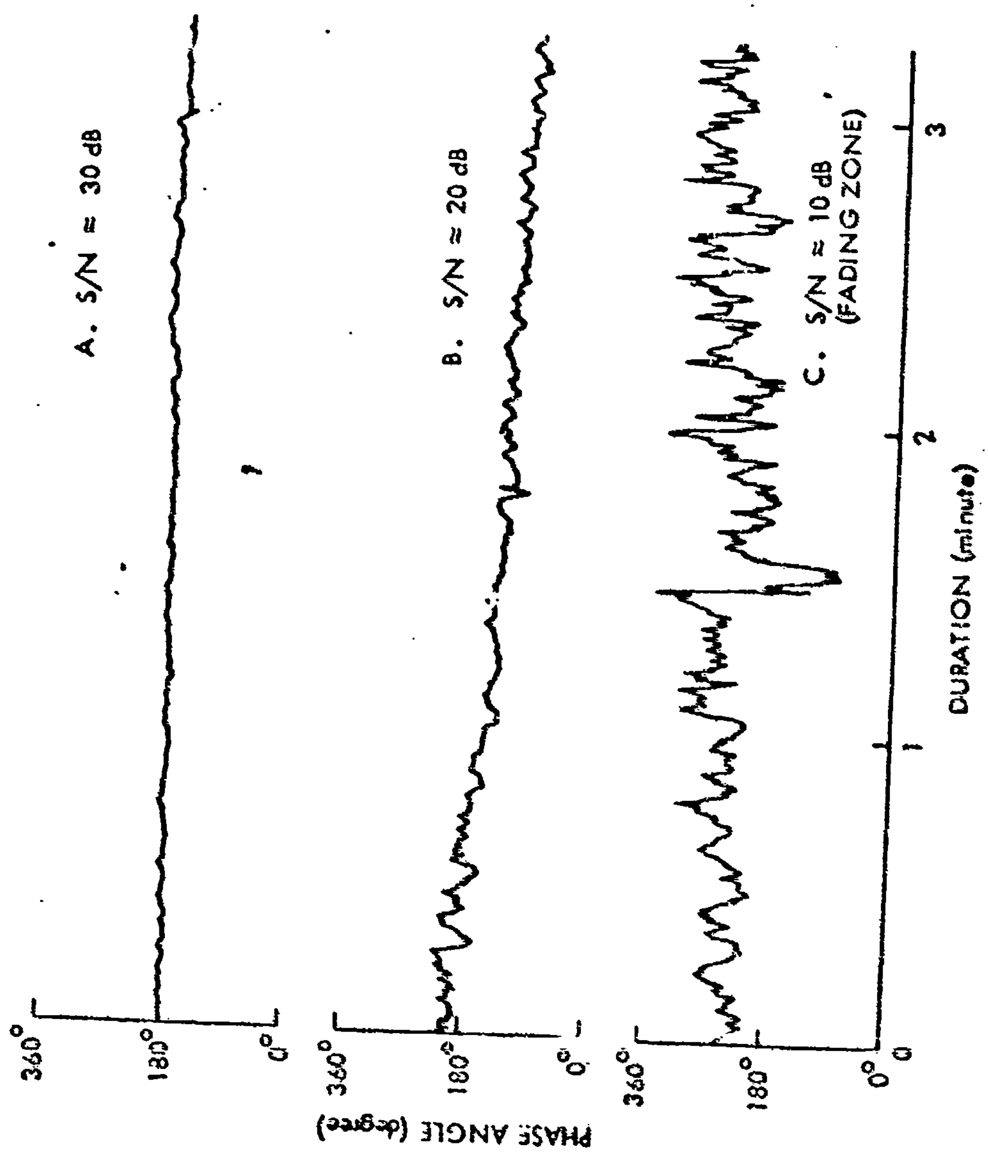

Fig 6. - Time Series of Relative Phase of Two Harmonically Related CW Signals

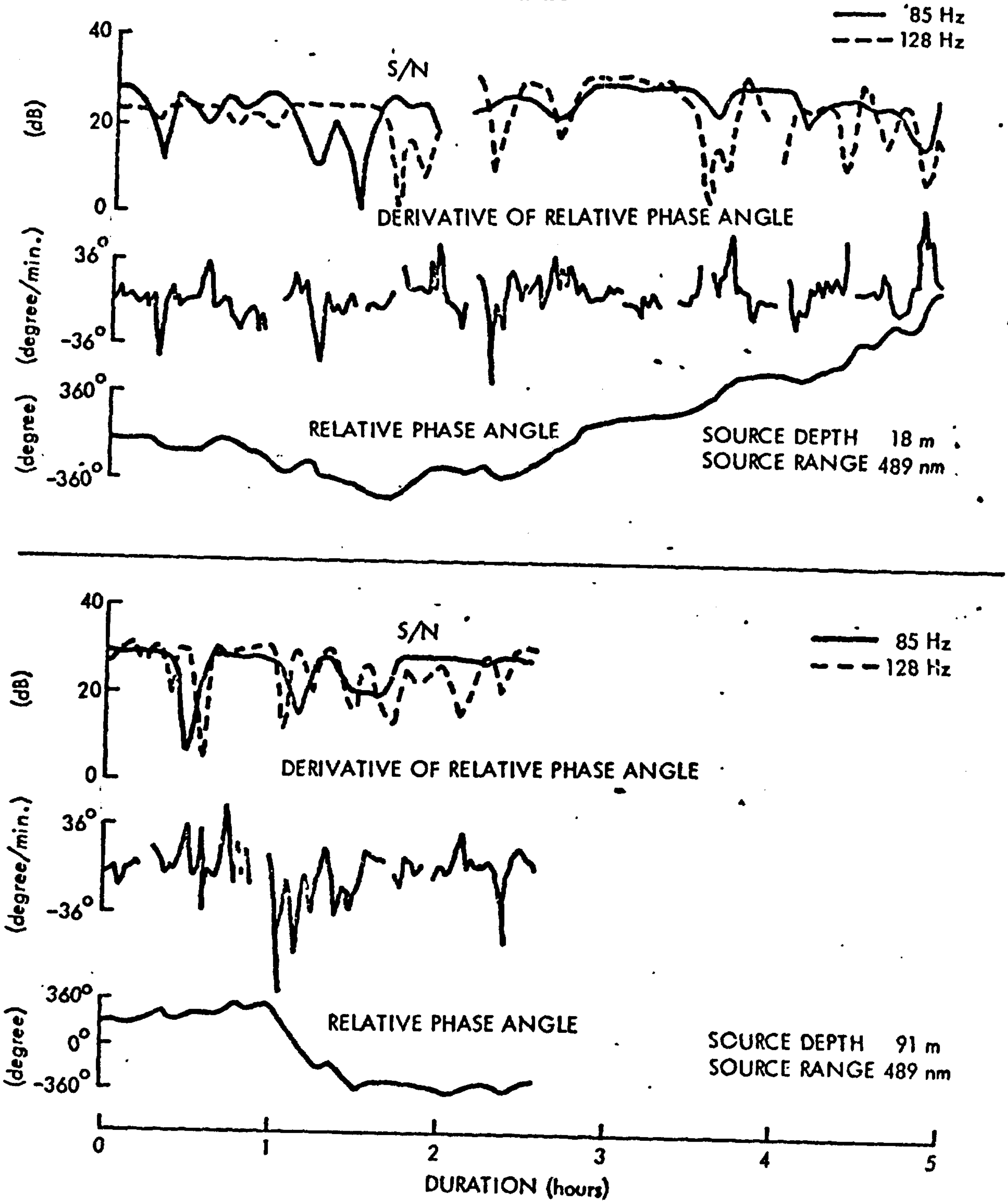

Fig 7. - Long Term Phase Angle Variation Measured at Station #1

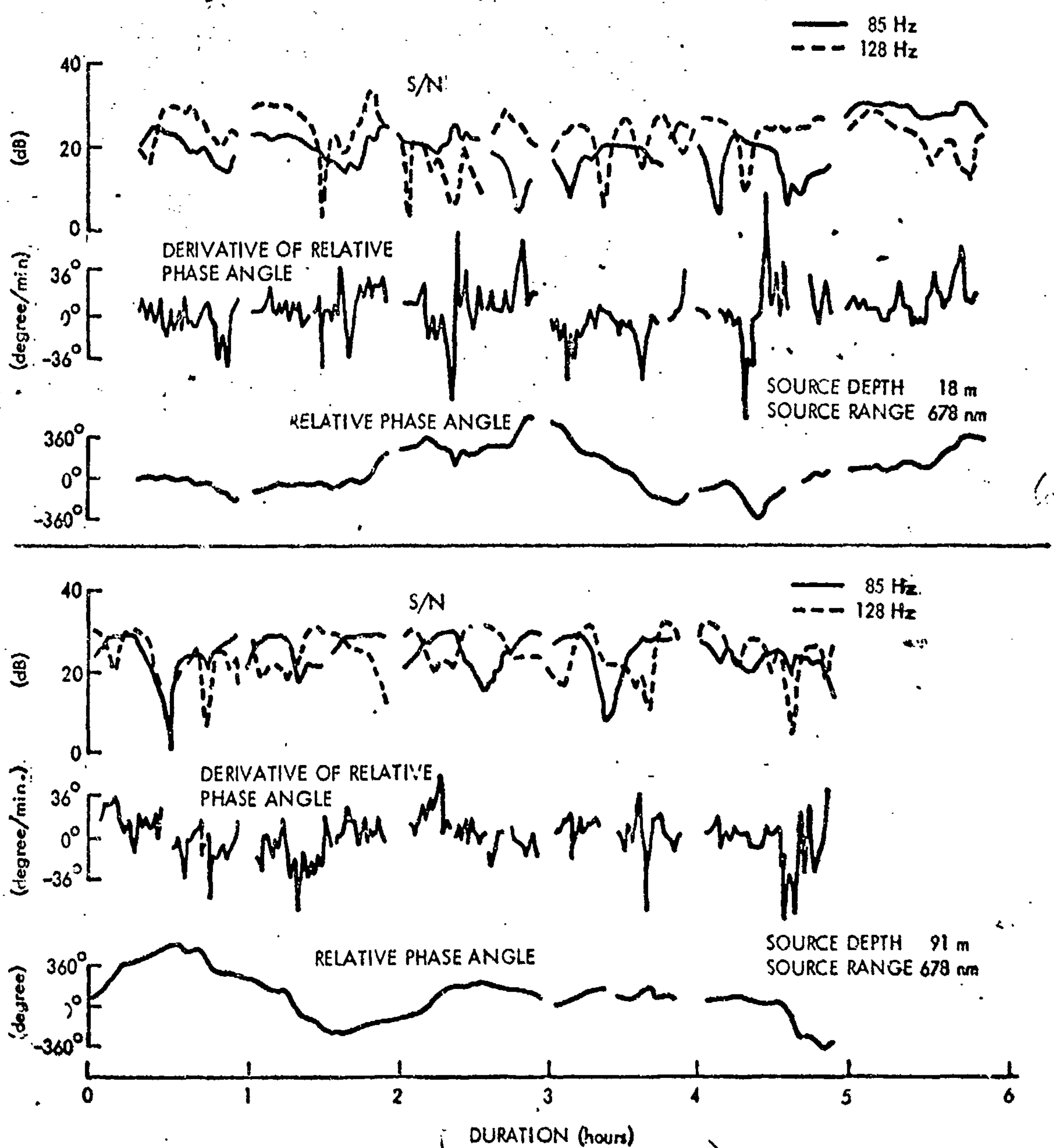

Fig 8. - Long Term Phase Angle Variation Measured at Station #3

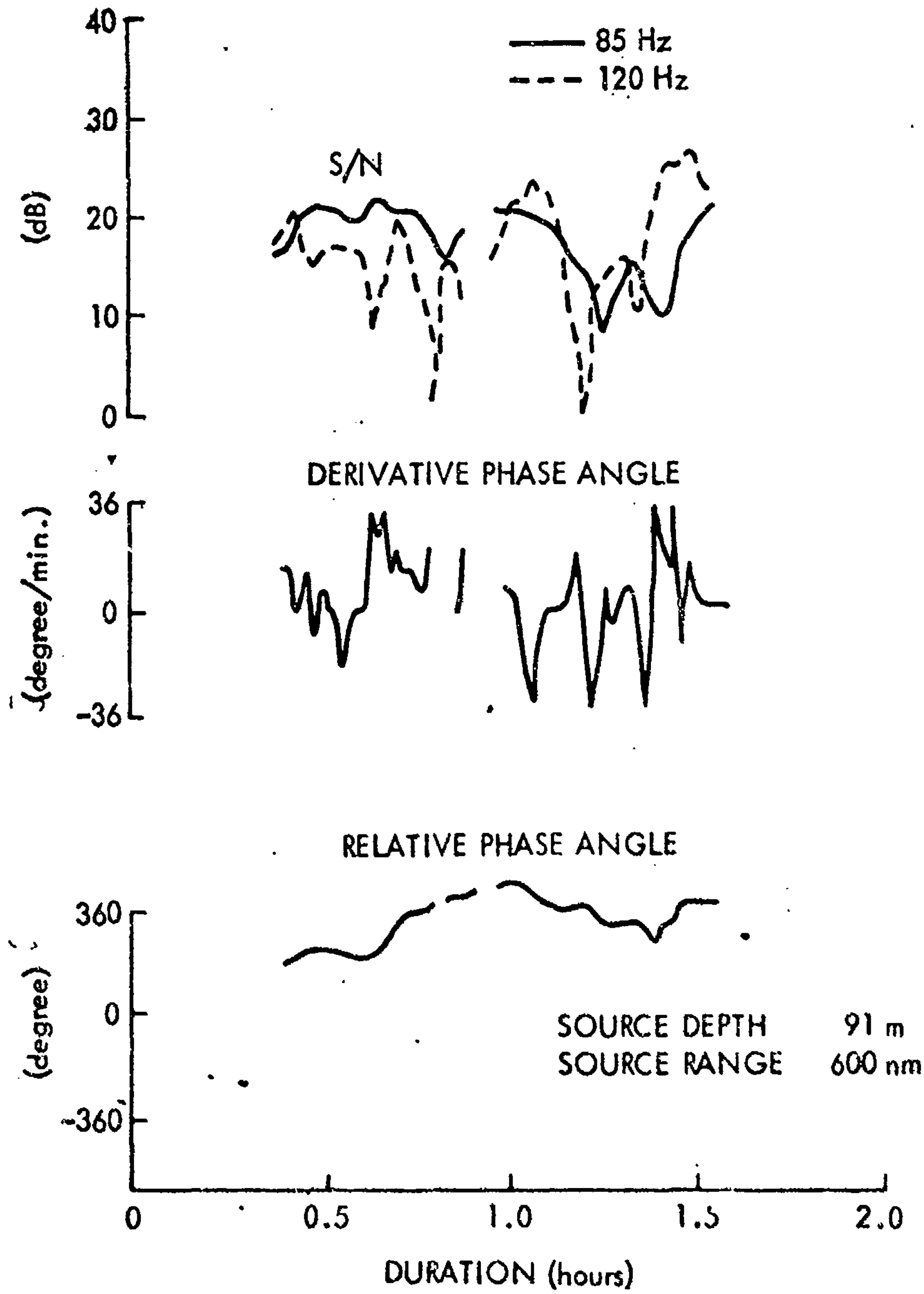

Fig 9. - Long Term Phase Angle Variation Measured at Station #4

Subj: Technical Memorandum; forwarding of (U)

Copy to:
Assistant Secretary of the Navy for Research and Development
Director, Defense, Research and Engineering (G. Cann)
Fleet Numerical Weather Central
COSL
CNR (Code 102-OS)
CNR (Code 102-OSC)
CNR (Code 400)
CNR (Code 412)
CNR (Code 480)
CNR (Code 486)
CNR (AESD)
CNM (NAVMAT 0341)
ARPA
MASWSP (ASW-10)
MASWSP (ASW-11)
MASWSP (ASW-14)
MASWSP (ASW-20)
MASWSP (ASW-111)
NAVSEA (SEA 09G32)
NAVSEA (SEA 06H1)
NAVSEA (SEA 06H1-4)
NAVAIRSYSCOM (AIR 540)
NAVAIRSYSCOM (AIR 50174)
NAVFACENGCOM (FPO-1E4)
NAVOCEANO (037)
NAVOCEANO (06)
NAVOCEANO (6130)
NAVELEX (320)

Subj: Technical Memorandum; forwarding of (U)

Copy to: (CONT)
NAVELEX (PME-124)
NAVELEX (PME-124T)
NAVELEX (PME-124TA)
NAVELEX (PME-124-20)
NAVELEX (PME-124-30)
NAVELEX (PME-124-40)
NAVELEX (PME-124-60)
NUC (Code 502)
NUC (Code 503)
NRL (Code 2627)
NRL (Code 8101)
NRL (Code 8167)
NRL (Code 8168)
NRL (Code 8170)
NADC (Code 205)
NSWC
NCSL
NSRDC
Center for Naval Analysis (CAPT Woods) **(Via CNO, OP-96L)**
ADL (Dr. G. Raisbeck) (Contract N000-14-72-C-0173)
TRW Systems, Inc. (R. Brown) (Contract N000-14-72-C-0227)
Planning Systems, Inc. (Dr. L. P. Solomon) (Contract N000-14-73-C-0233)
Undersea Research Corp. (J. Hess) (Contract N000-14-73-C-0484)
Underwater Systems, Inc. (Dr. M. Weinstein) (Contract N000-14-72-C-0464)
BTL (Contract N00039-75-C-0101)
B-K Dynamics, Inc. (A. E. Fadness) (Contract N000-14-71-C-0329)
TRACOR (J. T. Gottwald) (Contract N00014-71-C-0438)
Texas Instruments, Inc. (A. Kirst) (Contract N00014-71-C-0400)
RAFF Associates, Inc. (Dr. Julie Bowen) (Contract N00014-71-C-0118)
University of Miami (Dr. S. C. Daubin) (Contract N00014-67-A-0201-0024)
WHOI (Dr. E. E. Hays) (Contract N00014-71-C-0057)
Director, Marine Physical Lab, Scripps Institution of Oceanography, (Contract N00014-69-A-0200-6002)
Western Electric Company (Contract N00039-74-C-0193)
Seismic Engineering Co. (Contract N00014-73-C-0411)
BBN (D. Sachs) (Contract N00014-72-C-0499)
Tetra-Tech, Inc. (C. H. Dabney) (Contract N00014-71-C-0401)
Xonics, Inc. (S. Kulek) (Contract N00014-72-C-0418)
ARL at Austin (Dr. Loyd Hampton) (Contract N00014-72-C-0476)
NRL (Code 8160)
Naval Postgraduate School, Monterey, CA

DEPARTMENT OF THE NAVY
OFFICE OF NAVAL RESEARCH
875 NORTH RANDOLPH STREET
SUITE 1425
ARLINGTON VA 22203-1995

IN REPLY REFER TO:

5510/1
Ser 321OA/011/06
31 Jan 06

MEMORANDUM FOR DISTRIBUTION LIST

Subj: DECLASSIFICATION OF LONG RANGE ACOUSTIC PROPAGATION PROJECT (LRAPP) DOCUMENTS

Ref: (a) SECNAVINST 5510.36

Encl: (1) List of DECLASSIFIED LRAPP Documents

1. In accordance with reference (a), a declassification review has been conducted on a number of classified LRAPP documents.

2. The LRAPP documents listed in enclosure (1) have been downgraded to UNCLASSIFIED and have been approved for public release. These documents should be remarked as follows:

   Classification changed to UNCLASSIFIED by authority of the Chief of Naval Operations (N772) letter N772A/6U875630, 20 January 2006.

   DISTRIBUTION STATEMENT A: Approved for Public Release; Distribution is unlimited.

3. Questions may be directed to the undersigned on (703) 696-4619, DSN 426-4619.

BRIAN LINK
By direction

Subj: DECLASSIFICATION OF LONG RANGE ACOUSTIC PROPAGATION PROJECT (LRAPP) DOCUMENTS

DISTRIBUTION LIST:

NAVOCEANO (Code N121LC – Jaime Ratliff)
NRL Washington (Code 5596.3 – Mary Templeman)
PEO LMW Det San Diego (PMS 181)
DTIC-OCQ (Larry Downing)
ARL, U of Texas
Blue Sea Corporation (Dr.Roy Gaul)
ONR 32B (CAPT Paul Stewart)
ONR 321OA (Dr. Ellen Livingston)
APL, U of Washington
APL, Johns Hopkins University
ARL, Penn State University
MPL of Scripps Institution of Oceanography
WHOI
NAVSEA
NAVAIR
NUWC
SAIC

Declassified LRAPP Documents

Report Number	Personal Author	Title	Publication Source (Originator)	Pub. Date	Current Availability	Class.
Unavailable	Beam, J. P., et al.	LONG-RANGE ACOUSTIC PROPAGATION LOSS MEASUREMENTS OF PROJECT TRANSLANT I IN THE ATLANTIC OCEAN EAST OF BERMUDA	Naval Underwater Systems Center	740612	ADC001521	U
Unavailable	Cornyn, J. J., et al.	AMBIENT-NOISE PREDICTION. VOLUME 2. MODEL EVALUATION WITH IOMEDEX DATA	Naval Research Laboratory	740701	AD0530983	U
Unavailable	Unavailable	COHERENCE OF HARMONICALLY RELATED CW SIGNALS	Naval Underwater Systems Center	740722	ADB181912	U
Unavailable	Banchero, L. A., et al.	IOMEDEX SOUND VELOCITY ANALYSIS AND ENVIRONMENTAL DATA SUMMARY	Naval Oceanographic Office	740801	ADC000419	U
3810	Unavailable	CONSTRUCTION AND CALIBRATION OF USRD TYPE F58 VIBROSEIS MONITORING HYDROPHONES SERIALS 1 THROUGH 7	Naval Research Laboratory	741002	ND	U
ARL-TM-73-11; ARL-TM-73-12	Ellis, G. E., et al.	ARL PRELIMINARY DATA ANALYSIS FROM ACODAC SYSTEM; ANALYSIS OF THE BLAKE TEST ACODAC DATA	University of Texas, Applied Research Laboratories	741015	ADA001738; ND	U
Unavailable	Mitchell, S. K., et al.	QUALITY CONTROL ANALYSIS OF SUS PROCESSING FROM ACODAC DATA	University of Texas, Applied Research Laboratories	741015	ADB000283	U
Unavailable	Unavailable	MEDEX PROCESSING SYSTEM. VOLUME II. SOFTWARE	Bunker-Ramo Corp. Electronic Systems Division	741021	ADB000363	U
Unavailable	Spofford, C. W.	FACT MODEL. VOLUME I	Maury Center for Ocean Science	741101	ADA078581	U
Unavailable	Bucca, P. J., et al.	SOUND VELOCITY STRUCTURE OF THE LABRADOR SEA, IRMINGER SEA, AND BAFFIN BAY DURING THE NORLANT-72 EXERCISE	Naval Oceanographic Office	741101	ADC000461	U
Unavailable	Anderson, V. C.	VERTICAL DIRECTIONALITY OF NOISE AND SIGNAL TRANSMISSIONS DURING OPERATION CHURCH ANCHOR	Scripps Institution of Oceanography Marine Physical Laboratory	741115	ADA011110	U
Unavailable	Baker, C. L., et al.	FACT MODEL. VOLUME II	Office of Naval Research	741201	ADA078539	U
ARL-TR-74-53	Anderson, A. L.	CHURCH ANCHOR EXPLOSIVE SOURCE (SUS) PROPAGATION MEASUREMENTS (U)	University of Texas, Applied Research Laboratories	741201	ADC002497; ND	U
MCR106	Cherkis, N. Z., et al.	THE NEAT 2 EXPERIMENT VOL 1 (U)	Maury Center for Ocean Science	741201	NS; ND	U
MCR107	Cherkis, N. Z., et al.	THE NEAT 2 EXPERIMENT VOL 2 - APPENDICES (U)	Maury Center for Ocean Science	741201	NS; ND	U
Unavailable	Mahler, J., et al.	INTERIM SHIPPING DISTRIBUTION	Tetra, Tech, BB&N, & PSI	741217	ND	U
75-9M7-VERAY-R1	Jones, C. H.	LRAPP VERTICAL ARRAY- PHASE IV	Westinghouse Electric Corp.	750113	ADA008427; ND	U
AESD-TN-75-01	Spofford, C. W.	ACOUSTIC AREA ASSESSMENT	Office of Naval Research	750201	ADA090109; ND	U